

Marquette University
e-Publications@Marquette

Chemistry Faculty Research and Publications

Chemistry, Department of

4-1-2018

Insight into Solvent Coordination of an Iron Porphyrin Hydroxylamine Complex from Spectroscopy and DFT Calculations

Md. Hafizur Rahman
Marquette University

Michael D. Ryan
Marquette University, michael.ryan@marquette.edu

Accepted version. *European Journal of Inorganic Chemistry*, No. 16 (April 30, 2018): 1762-1765. DOI.
© 2018 Wiley. Used with permission.

Marquette University

e-Publications@Marquette

Chemistry Faculty Research and Publications/College of Arts and Sciences

This paper is NOT THE PUBLISHED VERSION; but the author's final, peer-reviewed manuscript. The published version may be accessed by following the link in the citation below.

European Journal of Inorganic Chemistry, Vol. 16 (April 30, 2018): 1762-1765. [DOI](#). This article is © Wiley and permission has been granted for this version to appear in [e-Publications@Marquette](#). Wiley does not grant permission for this article to be further copied/distributed or hosted elsewhere without the express permission from Wiley.

Insight into Solvent Coordination of an Iron Porphyrin Hydroxylamine Complex from Spectroscopy and DFT Calculations

Md. Hafizur Rahman

Chemistry Department, Marquette University, PO Box 1881, 53201 Milwaukee, WI,

Michael D. Ryan

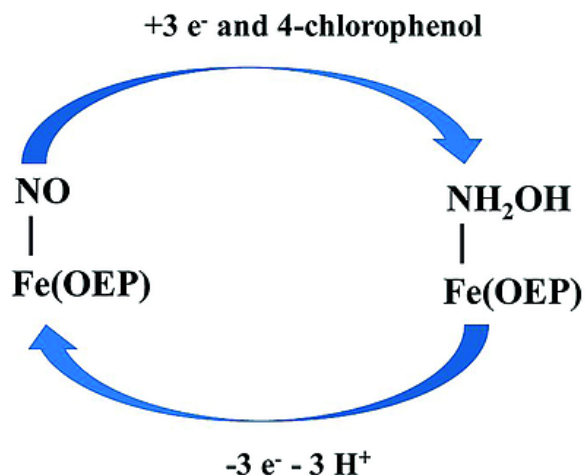
Chemistry Department, Marquette University, PO Box 1881, 53201 Milwaukee, WI,

Abstract

The reduction of Fe(OEP)(NO) in the presence of substituted phenols leads to a three-electron reduction to form Fe(OEP)(NH₂OH), which has been characterized by visible spectroscopy and electron stoichiometry. In this work, we have further characterized this species using infrared and ¹H NMR spectroscopy, along with DFT calculations. The infrared bands in the 3400–3600 cm⁻¹ region, due to hydroxylamine, were significantly downshifted to the 2500–2700 cm⁻¹ region when 4-[D₁]chlorophenol replaced the normal abundance acid. Using ¹H NMR spectroscopy, the hydroxylamine and the *meso*-protons were identified. From DFT calculations, the ¹H NMR spectra were most consistent with a six-coordinate complex, Fe(OEP)(NH₂OH)(THF).

Abstract

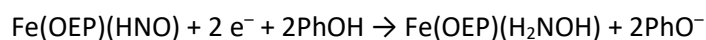
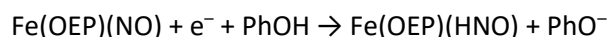
A ferrous porphyrin hydroxylamine complex can be generated using both chemical and electrochemical methods. This complex was characterized using visible, infrared, and ^1H NMR spectroscopy techniques and DFT calculations. The complex was found to be low-spin, and the spectroscopic and DFT data support the solvent, THF, as the most likely sixth ligand.



Introduction

Hydroxylamine is an important intermediate in many enzymatic systems in the nitrogen cycle. It is a presumed intermediate in the reduction of nitrite to ammonia by siroheme or cytochrome c nitrite reductases,¹ and is a substrate for hydroxylamine oxidoreductases.² In addition to hydroxylamine oxidoreductase, hydroxylamine has been found to bind to *A. ramosus* peroxidase.³ Recently hydroxylamine has been identified as the product of the electrochemical reduction of Fe(OEP)(NO) (OEP = octaethylporphyrin) in the presence of 2,6-dichlorophenol (dcp) using visible spectroelectrochemistry.⁴ While the spectral identification was consistent with the voltammetric data, the spectroscopic characterization was limited. It is the aim of this report to provide a more detailed spectral characterization. Bis(hydroxylamine) complexes of ferrous porphyrins have been previously characterized at reduced temperatures.⁵ At room temperature, the bis(hydroxylamine) ferrous porphyrin complex will undergo reductive nitrosylation to form Fe(OEP)(NO).⁶ Stable ferrous porphyrin *N*-alkyl hydroxylamine complexes have been reported.⁷ On the other hand, ferric "picket-fence" porphyrins will react with *O*-alkyl hydroxylamine to form a bis(ammonia) ferrous complex rather than a ferrous-nitrosyl species.⁸ Hydroxylamine itself was found to disproportionate in the presence of water-soluble ferric porphyrins to form NH_3 and N_2O .⁹

The reduction of Fe(OEP)(NO) in THF occurs in two one-electron steps with the formation of Fe(OEP)(NO)⁻ and Fe(OEP)(NO)²⁻.¹⁰ The spectroscopic properties of Fe(OEP)(NO)⁻ have been obtained as well as an X-ray structure.^{10, 11} In the presence of weak acids, such as substituted phenols, Fe(OEP)(NO)⁻ can be protonated to form Fe(OEP)(HNO), and be further reduced to Fe(OEP)(NH₂OH). The overall reaction can be written as:



where PhOH is a substituted phenol. The initial identification of the hydroxylamine product was based on the observed current in pulse polarography and visible spectroscopy.^{4, 12}

Results and Discussion

The visible spectroelectrochemistry of Fe(OEP)(NO) in 50 mM 4-chlorophenol is shown in Figure S1. As observed for the reduction of Fe(OEP)(NO) with 2,6-dcp previously, further reduction of Fe(OEP)(NO)⁻ occurred, rapidly forming a Fe(OEP)(NH₂OH) complex,⁴ with a sharp Soret band typical of low-spin ferrous porphyrins. Analysis of the reduction by evolving factor analysis showed that only two species were present during the reduction under these conditions (Figure S2). At this concentration of 4-chlorophenol, the intermediate, Fe(OEP)(HNO), was not observed. If the potential was then step to 0.0 V vs. Ag/AgNO₃, the complex was re-oxidized to Fe(OEP)(NO) (Figure S3). As was previously observed,⁴ the rate of oxidation was considerably slower than the reduction.

The infrared spectroelectrochemistry of Fe(OEP)(NO) in the presence of 4-chlorophenol is shown in Figure 1. In the absence of 4-chlorophenol, no bands were observed between 3450 and 3600 cm⁻¹. In the presence of 4 mM 4-chlorophenol (Figure 1, red trace) and at potentials just negative of the *E*^o for Fe(OEP)(NO), no bands were observed in that same region. Under these conditions, Fe(OEP)(NO) was reduced (Figure 1, 1671 cm⁻¹ band) and Fe(OEP)(HNO) was formed.⁴ DFT calculations of Fe(OEP)(HNO) showed that the ν_{HNO} band was predicted to be 2967 cm⁻¹. This band would not be visible due to a series of C–H vibrations which were present in that region. At 50 mM 4-chlorophenol and more negative potentials, Fe(OEP)(H₂NOH) was formed based on visible spectroelectrochemistry. When infrared spectroelectrochemistry was carried out at 100 mM 4-chlorophenol, two new bands were observed at 3465 and 3540 cm⁻¹. (Figure 1, brown, black, red traces with increasing time). The 3465 cm⁻¹ was obscured at longer times due to the decrease in the 4-chlorophenol band at 3263 cm⁻¹. The results are summarized in Table 1. The DFT results are in reasonable agreement with the experimental values, though the third DFT band overlapped too much with the 4-chlorophenol band to be observed. The question remains as to the actual structure of the complex. While Fe(OEP)(NO) is five-coordinate, the ferrous complexes formed may be six-coordinate with THF as the sixth ligand. The differences in Table 1 between the 5- and six-coordinate species were not large enough to make an unambiguous determination.

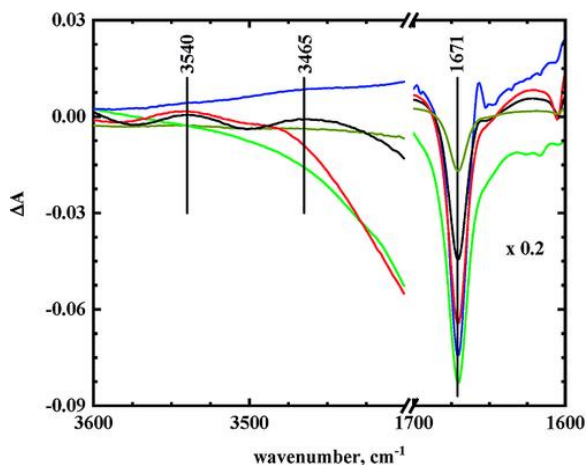


Figure 1. FTIR spectroelectrochemistry of Fe(OEP)(NO). Reduction of Fe(OEP)(NO) in 4-chlorophenol (initial: brown, intermediate: black, final: red). Reduction of Fe(OEP)(NO) in 4-[D₁]chlorophenol (blue). Fe(OEP)(HNO) generated electrochemically (green).

Table 1. Experimental and DFT calculated infrared bands for metalloporphyrin hydroxylamine complexes. For DFT calculations, first number is for Fe(OEP)(NH₂OH); second number is for Fe(OEP)(NH₂OH)(THF). Solvent: THF with 0.10 m TBAP

Solution	ν_{exp}	ν_{DFT}
		5-coord./6-coord.
Fe(OEP)(NO)/	—	3387/3286

4-chlorophenol	3465	3409/3386
	3540	3580/3667
Fe(OEP)(NO)/	–	2390/2372
4-[D ₁]chlorophenol	2587	2502/2503
	2649	2600/2671
Co(OEP)(NH ₂ OH) ₂ ⁺	3621	–
	3683	–

Figure 1 shows that Fe(OEP)(NO), in the presence of 4-chlorophenol, was not regenerated by a disproportionation reaction between Fe(OEP)(HNO) to form Fe(OEP)(NO) and H₂. This can occur at longer times but not on this time-scale.^{10, 13} In addition, no bands were observed for N₂O, another possible side reaction.

In order to confirm the origin of the observed bands, the experiment was then repeated with 4-[D₁]chlorophenol. The bands at 3465 and 3540 cm⁻¹ disappeared (Figure 1, blue). The experiment was then repeated with 0.10 m 4-[D₁]chlorophenol. The results are shown in Figure S4. The spectrum in the 2500–2700 cm⁻¹ region was similar the spectrum for normal abundance 4-chlorophenol except that the bands were shifts from the 3400–3600 cm⁻¹ region to the 2500–2700 cm⁻¹ region. Two bands were observed at 2587 and 2649 cm⁻¹, and a large negative band was observed at 2428 cm⁻¹, due to the reduction of the phenolic group in 4-[D₁]chlorophenol. The isotopic shifts were consistent with the replacement of ¹H with ²H, and was confirmed by the shift in the phenol band for 4-chlorophenol (3263 to 2428 cm⁻¹).

Further identification of the Fe(OEP)(NH₂OH) complex was done using ¹H NMR spectroscopy. The complex was synthesized by anthracenide reduction in the presence of 4-[D₄]chlorophenol. Because of the large excess of 4-chlorophenol, deuterated substrates were used to see the proton resonances for the iron complex. The ¹H NMR spectrum is shown in Figure 2. Resonances for the hydroxylamine were observed at –2.90 and –9.70 ppm. These results were similar to Co(OEP)(NH₂OH)₂⁺. These chemical shifts are consistent with low-spin ferrous complexes. When 4-[D₄]chlorophenol was replaced with 4-[D₅]chlorophenol, these resonances disappeared (Figure 2). The results are summarized in Table 2. Further reduction of hydroxylamine to ammonia, as was observed by McQuarters et al.,⁸ was not consistent with the data. First, two resonances are observed for the ligand in the NMR spectrum, as was observed for the cobalt complex. Second, both H–O and H–N vibrations are present in the infrared. Finally, the complex can be oxidized back to Fe(OEP)(NO), which would be unlikely for the ammonia complex.

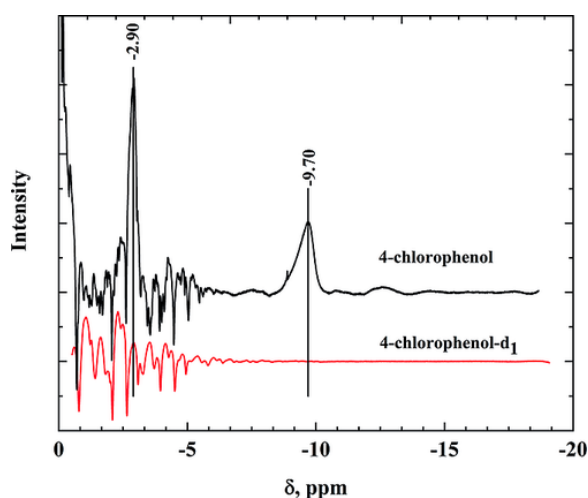


Figure 2 ¹H NMR spectra for the chemically synthesized Fe(OEP)(NH₂OH) complex. Black line corresponded to the use of 4-[D₄]chlorophenol; Red line 4-[D₅]chlorophenol.

Table 2. Experimental and DFT calculated resonance for the hydroxylamine ligand in metalloporphyrin-hydroxylamine complexes. All DFT calculations are for S = 0 complexes

Compound		δ [ppm]	δ [ppm]
Fe(OEP)(NH ₂ OH)	Exp.	-2.90	-9.70
	DFT	-14.37	-42.24
Fe(OEP)(NH ₂ OH)(THF)	DFT	-3.92	-10.23
Co ^{III} (OEP)(NH ₂ OH) ₂ ⁺	Exp.	0.06	-2.22

Because the iron was more displaced from the porphyrin plane for the Fe(OEP)(NH₂OH) (0.095 Å) complex as compared to the Fe(OEP)(NH₂OH)(THF) complex (0.016 Å), the six coordinate complex was most consistent with the experimental values. The DFT calculated structures for Fe(OEP)(NH₂OH) and Fe(OEP)(NH₂OH)(THF) are shown in Figure S5.

Generally low-spin ferrous porphyrin complexes are six-coordinate rather than five-coordinate, except when strong π -ligands such as NO are present. In addition to the axial hydroxylamine ligand, the *meso*-protons for Fe(OEP)(NH₂OH)(THF) are also shifted from their normal positions. Using Fe(OEP)(NO) and Fe([D₄]OEP)(NO), it was possible to identify the *meso* resonances. For normal abundance Fe(OEP)(NO), the hydroxylamine complex had a resonance at $\delta = 15.15$ ppm, which was missing when one started with Fe([D₄]OEP)(NO). In this case, DFT calculations predict that the six-coordinate complex would have *meso* resonance at $\delta = 11.38$ ppm, while the five-coordinate was predicted to have *meso*-resonances at $\delta = 15.80$ ppm. While the five-coordinate species was closer to the observed value, the differences in this case are not large, as observed with the hydroxylamine resonances. Overall, the data supports a six-coordinate ferrous porphyrin complex with ligation by hydroxylamine and THF.

Mechanisms for the decomposition of the ferrous-hydroxylamine complexes generally involve the presence of excess hydroxylamine with a bis(hydroxylamine) complex.^{8, 9} The excess hydroxylamine initiates a radical reaction on the complex, which is followed by an internal disproportionation to eventually lead to the ferrous nitrosyl.⁸ This mechanism cannot occur with the complex described in this report, as only a mono complex was formed and there was no excess hydroxylamine.

Conclusions

In summary, Fe(OEP)(NO) can be reduced to Fe(OEP)(NH₂OH)(THF) in THF with a strong reductant and a weak acid such as chlorophenols. The structure was deduced using DFT calculations and UV/Visible, infrared and ¹H NMR spectroscopy.

Experimental Section

Chemicals: Tetrabutylammonium perchlorate (TBAP), iron(III) octaethylporphyrin (FeOEP), sodium methoxide and hydroxylamine hydrochloride were purchased from Sigma–Aldrich Chemical Co. 4-[D₄]Chlorophenol and 4-[D₅]chlorophenol purchased from CDN isotopes. TBAP was dried at 90 °C under a vacuum overnight before use. Anhydrous THF was refluxed in the presence of sodium metal and benzophenone until the solution was a persistent dark blue color. After purification, the solvent was collected under argon and stored in the glove box. 4-Chlorophenol was purified by sublimation. The iron-porphyrin nitrosyl and nitroxyl complexes were synthesized by literature methods.^{6, [11]} The generation of Fe(OEP)(NH₂OH) was carried out by the reduction of Fe(OEP)(NO) with anthracene in the presence of 4-chlorophenol (see Supporting Information for additional details).

Procedures: UV/Visible and FTIR spectroelectrochemical experiments were carried out using one of two methods depending upon the solution. For UV/Visible spectra, a slow cyclic scan of the potential was sufficient to insure complete electrolysis at each potential. For the FTIR (except as noted), potentials were chosen to be sufficiently negative to insure complete electrolysis.

Instrumentation: Spectroelectrochemical (SEC) experiments used a low-volume thin layer quartz glass cell purchased from BAS Inc. A platinum mesh was used as the working electrode and a platinum wire was used as the auxiliary electrode. Potentials were measured relative to the Ag/AgNO₃ (in CH₃CN) reference electrode. The UV/Visible spectra were recorded on a HP 8452A diode array spectrophotometer. The FTIR spectroelectrochemical cell was described previously.^[11] The infrared spectra were obtained using 64 scans and 2 cm⁻¹ resolution, recorded with a Thermo Nicolet-FTIR spectrophotometer (Model 670 Nexus) with a MCT detector. ¹H-NMR spectroscopy measurements were performed using a Bruker Avance IIIHD 600 MHz spectrometer (Medical College of Wisconsin).

Computational Methods: Electronic structure calculations were carried out with the Gaussian 09 suite of programs¹⁴ using the m06 DFT functional and the TZVP basis set for all elements except for iron, and a scale factor of 0.94 was used for the infrared energies. The Wachters' basis set was used for iron.¹⁵ All calculations converged using the tight optimization criteria. Evolving factor analysis was carried out with MATLAB and PLS_TOOLBOX.

Acknowledgements

The authors would like to thank the Medical College of Wisconsin for their help in obtaining the NMR spectra.

References

- 1a) Vega, J. M. and Kamin, H., *J. Biol. Chem.*, 1977, **252**, 896– 909; b) Einsle, O., Messerschmidt, A., Huber, R., Kroneck, P. M. H. and Neese, F., *J. Am. Chem. Soc.*, 2002, **124**, 11737– 11745; c) Nakano, S., Takahashi, M., Sakamoto, A., Morikawa, H. and Katayanagi, K., *Proteins Struct., Funct., Bioinf.*, 2012, **80**, 2035– 2045.
- 2 Hooper, A. B. and Terry, K. R., *Biochim. Biophys. Acta*, 1979, **571**, 12– 20.
- 3 Wariishi, H., Nonaka, D., Johjima, T., Nakamura, N., Naruta, Y., Kubo, S. and Fukuyama, K., *J. Biol. Chem.*, 2000, **275**, 32919– 32924.
- 4 Rahman, M. H. and Ryan, M. D., *Inorg. Chem.*, 2017, **56**, 3302– 3309.
- 5 Feng, D. and Ryan, M. D., *Inorg. Chem.*, 1987, **26**, 2480– 2483.
- 6 Choi, I.-K., Liu, Y. M., Wei, Z. and Ryan, M. D., *Inorg. Chem.*, 1997, **36**, 3113– 3118.
- 7 Newman, A. R. and French, A. N., *Inorg. Chim. Acta*, 1987, **129**, L37– L39.
- 8 McQuarters, A. B., Goodrich, L. E., Goodrich, C. M. and Lehnert, N., *Z. Anorg. Allg. Chem.*, 2013, **639**, 1520– 1526.
- 9 Bari, S. E., Amorebieta, V. T., Gutiérrez, M. M., Olabe, J. A. and Doctorovich, F., *J. Inorg. Biochem.*, 2010, **104**, 30– 36.
- 10 Choi, I.-K., Liu, Y., Feng, D., Paeng, K. J. and Ryan, M. D., *Inorg. Chem.*, 1991, **30**, 1832– 1839.
- 11a) Kundakarla, N., Lindeman, S., Rahman, M. H. and Ryan, M. D., *Inorg. Chem.*, 2016, **55**, 2070– 2075; b) Wei, Z. and Ryan, M. D., *Inorg. Chem.*, 2010, **49**, 6948– 6954.
- 12 Liu, Y. M. and Ryan, M. D., *J. Electroanal. Chem.*, 1994, **368**, 209– 219.
- 13 Goodrich, L. E., Roy, S., Alp, E. E., Zhao, J., Hu, M. Y. and Lehnert, N., *Inorg. Chem.*, 2013, **52**, 7766– 7780.
- 14 Frisch, M. J., Trucks, G. W., Schlegel, H. B., Scuseria, G. E., Robb, M. A., Cheeseman, J. R., Scalmani, G., Barone, V., Mennucci, B., Petersson, G. A., Nakatsuji, H., Caricato, M., Li, X., Hratchian, H. P., Izmaylov, A. F., Bloino, J., Zheng, G., Sonnenberg, J. L., Hada, M., Ehara, M., Toyota, K., Fukuda, R., Hasegawa, J., Ishida, M., Nakajima, T., Honda, Y., Kitao, O., Nakai, H., Vreven, T., Montgomery, J. A., Peralta, J.

E., Ogliaro, F., Bearpark, M., Heyd, J. J., Brothers, E., Kudin, K. N., Staroverov, V. N., Kobayashi, R., Normand, J., Raghavachari, K., Rendell, A., Burant, J. C., Iyengar, S. S., Tomasi, J., Cossi, M., Rega, N., Millam, J. M., Klene, M., Knox, J. E., Cross, J. B., Bakken, V., Adamo, C., Jaramillo, J., Gomperts, R., Stratmann, R. E., Yazyev, O., Austin, A. J., Cammi, R., Pomelli, C., Ochterski, J. W., Martin, R. L., Morokuma, K., Zakrzewski, V. G., Voth, G. A., Salvador, P., Dannenberg, J. J., Dapprich, S., Daniels, A. D., Farkas, Ö., Foresman, J. B., Ortiz, J. V., Cioslowski, J. and Fox, D. J., Gaussian 09, Revision ABCD.0123, Gaussian, Inc., Wallingford CT, 2009.

15 Wachters, A. J. H., *J. Chem. Phys.*, 1970, **52**, 1033– 1036.

Eur. J. Inorg. Chem. · ISSN 1099–0682

<https://doi.org/10.1002/ejic.201800040>

SUPPORTING INFORMATION

Title: Insight into Solvent Coordination of an Iron Porphyrin Hydroxylamine Complex from Spectroscopy and DFT Calculations

Author(s): Md. Hafizur Rahman, Michael D. Ryan*

Table of Contents:

Synthesis of Fe(OEP)(NH ₂ OH)	3
Figure S1. Visible spectroelectrochemistry of Fe(OEP)(NO) in the presence of 4-chlorophenol	4
Figure S2. Evolving factor analysis for the reduction of Fe(OEP)(NO) in the presence of 4-chlorophenol .	5
Figure S3. Re-oxidation of Fe(OEP)(NH ₂ OH) at 0.00 V vs Ag/AgNO ₃	6
Figure S4. Infrared spectroelectrochemistry of Fe(OEP)(NO) in 100 mM 4-chlorophenol and 4- chlorophenol-d1	7
Figure S5. DFT calculated structures for Fe(OEP)(NH ₂ OH) and Fe(OEP)(NH ₂ OH)(THF)	8

Synthesis of Fe(OEP)(NH₂OH):

Reducing agent. Fifty-five mg of cryptand and 27 mg of anthracene was placed in 25 mL round bottle flask. To the flask, five mL of double distilled THF was added. A small piece of potassium metal (which was rinsed with hexane and dried) was then added to the solution. The solution was stirred 3-4 hours until the solution turns dark blue color.

In a vial, 15-25 mg of very pure Fe(OEP)(NO) [The Fe(OEP)(NO) was washed with methanol to remove extra NH₂OH] was added with a micro stirrer. One-two mL of reducing agent was added to the vial and stirred for 30 minutes. The reduction was checked by UV-visible spectrum. Then 100-200 mM of 4- chlorophenol (for 2,3-dcp and 2,6-dcp 50 mM) was added to the Fe(OEP)(NO)- solution. The spectrum was taken within 2-3 minutes. For NMR spectra, the solution was inserted in the NMR tube and frozen in liquid nitrogen within 1-2 minutes. All operations were carried out in a glove box. Visible bands at 406, 526 and 556 nm were observed, which were consistent with the spectroelectrochemically obtained spectra.

Figure S1. Visible spectroelectrochemistry of Fe(OEP)(NO) in the presence of 4-chlorophenol. Initial spectrum (black); intermediate spectra (green, E = -0.578, -0.608, -0.644, -0.686 and -0.734 V); final spectrum (blue, E = -0.800 V). Solvent: THF. 0.10 M TBAP.

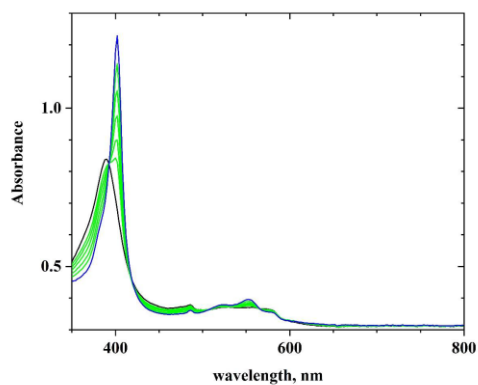


Figure S2. Evolving factor analysis for the reduction of Fe(OEP)(NO) in the presence of 4-chlorophenol. $E_{\text{initial}} = -0.500$ V and $E_{\text{final}} = -0.800$ V. Solvent: THF with 0.10 M TBAP. The appearance of the third factor at longer times is an artifact due to deviations from Beer's Law for the strong Soret band and the low resolution (2 nm) of the diode array spectrophotometer.

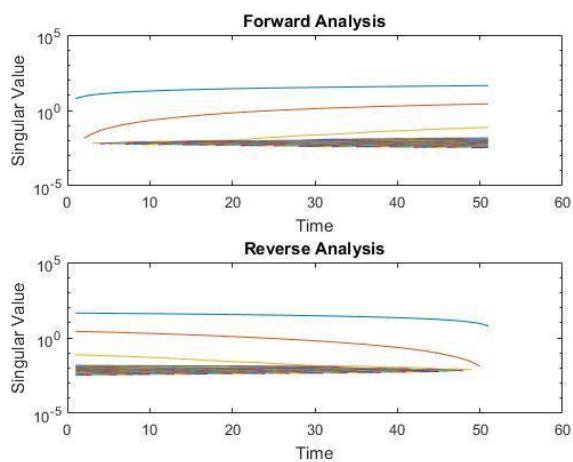


Figure S3. Re-oxidation of Fe(OEP)(NH₂OH) at 0.00 V vs Ag/AgNO₃. Time after potential stepped to 0.00 V: 451 s (black), 757 s, 938 s, 1118 s, 1418s, 2200 s and 2998 s (blue). Intermediate spectra are green. Solvent: THF with 0.10 M TBAP.

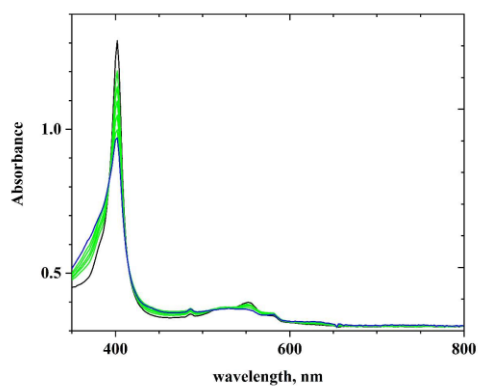


Figure S4. Infrared spectroelectrochemistry of Fe(OEP)(NO) in 100 mM 4-chlorophenol and 4-chlorophenol-d1. Formation of Fe(OEP)(NH2OH): 4-chlorophenol-d1 (green), 4-chlorophenol (black, brown, blue); Formation of Fe(OEP)(HNO) with 4-chlorophenol (red)

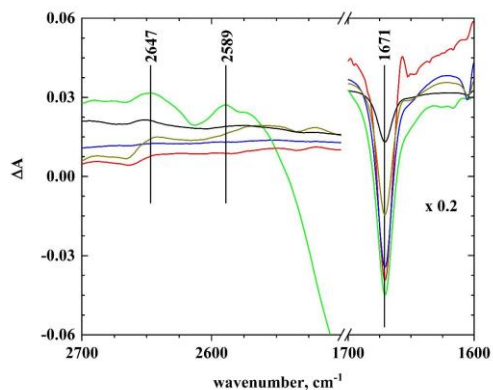


Figure S5. A. DFT calculated structure for Fe(OEP)(NH2OH). B. DFT calculated structure for Fe(OEP)(NH2OH)(THF). A. B.

